sciendo

LATVIAN JOURNAL OF PHYSICS
AND TECHNICAL SCIENCES
2022, N 5

DOI: 10.2478/lpts-2022-0041

POTENTIAL DECAY SIMULATION ON INSULATING FILMS

S. Kasri[1], L. Herous[1], K. Smili[1,2], M. T. Kimour[3], A. Dekhane[1*]

[1] Laboratory of Electromechanical Engineering,
University of Badji Mokhtar,
B.P.12, Sidi Amar, Annaba, 23220, ALGERIA
[2] Higher School of Industrial Technologies,
Safsaf city, BP 218, Annaba, 23000, ALGERIA
[3] Laboratory of Embedded Systems Research (LASE),
University of Badji Mokhtar,
B.P.12, Sidi Amar, Annaba, 23220, ALGERIA
*e-mail: a.dekhane@esti-annaba.dz

Surface potential decay (SPD) of a corona charged polymeric material is a powerful tool to characterise electrical properties such as charge transport, trapping/detrapping and recombination. Over the years, various predictive simulation techniques have been proposed to describe charge transport within the material. Despite recent progress, it appears that there have been a few attempts to theoretically interpret the nature of the charge migration on the insulation surface. The aim of the present paper is to introduce a new technique with differential evolution algorithm (DEA) to reveal the steady state surface potential decay experimental results. Experimental measurement was carried on a thin film of polyethylene terephthalate (thickness: 0.5 mm; surface: 50 mm x 50 mm). The domains of variation of the factors used were respectively: 1000 V to 1800 V; 25 to 55 °C; 50 % to 80 %. The simulation results show that computational modelling and optimization approaches may improve the effectiveness to characterise electrical properties of polymers. More importantly, these studies demonstrate that DEA is effective and performs better than the experimental design method.

Keywords: Differential evolution algorithm, genetic algorithms, polymers, simulation, surface potential decay.

1. INTRODUCTION

Synthetic insulating polymers are widely applied in electrical industry due to their excellent electrical, thermal, and mechanical properties. In many cases, such polymers are used in hostile environments where they may be subjected to attack by non-ionizing radiations, water, corrosive materials, etc. Therefore, their properties are deteriorated and a premature ageing of the electrical insulation can be observed.

The measurement of the isothermal surface potential decay after charge deposition provides a convenient method to investigate the electrical properties of such insulating materials. The main fields of industry source of numerous works on surface potential decay are electro optics (photocopies and laser printers), electret materials and electrical industry for the development of insulating polymers for high voltage insulation [1]–[4].

During the past two decades, many theories have been developed in order to explain the kinetics of surface potential decay. In a previous paper [5]–[8], experimental measurements on 500 mm thick polyethylene terephthalate (PET) samples pointed out that the surface potential decay is influenced by several factors, including the initial potential *V0*, the duration *tc* of the exposure to the corona discharge, the ambient temperature θ, and the relative humidity *RH*.

The design of experiment methodology has been recently used to optimize the process by evaluating instantaneously the effects of some factors and their interactions on the process [9]. Recently, modelling surface potential decay of polymer (PET) by artificial neuron networks [10]–[12] has been employed for modelling this phenomenon. The main objective of the present study is to assess the applicability of a new technique with differential evolution algorithm (DEA) to reveal the steady state surface potential decay experimental results. The novelty of this methodology is that it proposes a factorial experimentation, in which the factors investigated vary simultaneously. Simple mathematical processing of experimental design data enables a rather accurate evaluation of factor effects and interactions. Experimental design can also be used for determining the relationship between the factors affecting a process and the output of that process.

2. EXPERIMENTAL DETAILS

The surface potential decay experiment is described in Fig. 1 [6], [8].

The samples with one surface held firmly on to an earthed metal plate electrode and the other free surface were used. They might be charged on their free surface by exposure to a corona point discharge situated above the surface and behind a grid electrode. The grid was a fine metal mesh situated above the sample surface so that a reasonably uniform field might be generated in the gap between the grid and the PET surface [13], [14].

By selecting an appropriate corona point and grid potential *Vp* and *Vg*, respectively, it was possible to charge the polymer surface with ions of either sign and to a potential value limited by the grid potential *Vg*.

After charging the turntable was rotated under a non-contacting probe. The probe

was connected to an electrostatic voltmeter (Monroe type), which transmitted data to the computer. The surface potential was then measured and continuously recorded. All operations were controlled by a computer.

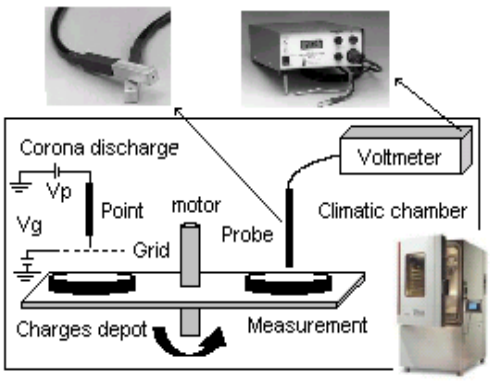


Fig. 1. Equivalent electrical circuit of photovoltaic module.

All the measurements of surface potential decay were carried out in situ, in a commercial climatic chamber, in which humidity and temperature were controlled. Experimental measurement was carried out on a thin film of polyethylene terephthalate (thickness: 0.5 mm; surface: 50 mm x 50 mm). The domains of factors variation used were respectively:

- Initial potential V_0: -1000 to -1800 V.
- Ambient temperature **θ:** 20 to 55 °C.
- Relative humidity RH: 50 % to 80 %.

A typical family of *V(t)* curves obtained [6] after negative corona at various grid potentials, under similar ambient conditions (T= 55 °C, RH= 50 %) can be examined in Fig. 2. A fast-initial decay of the potential can be noticed in all cases, as well as the so-called cross-over phenomenon [15], [16]; the samples initially charged to a higher potential displayed a more rapid potential decay than those charged to a lower potential. The fast-initial decay of the surface potential might be attributed to the partial injection of deposited charges into the polymer bulk under the electrical field generated by the charges themselves, and this trend was enhanced by raising V_0. Once injected into the bulk, the charges are expected to drift towards the ground electrode under the influence of this field. Therefore, the initial potential V_0 has a stronger effect right on the short-term decay rate $D_{500\,s}$ than on the long-term decay rate $D_{3000\,s}$.

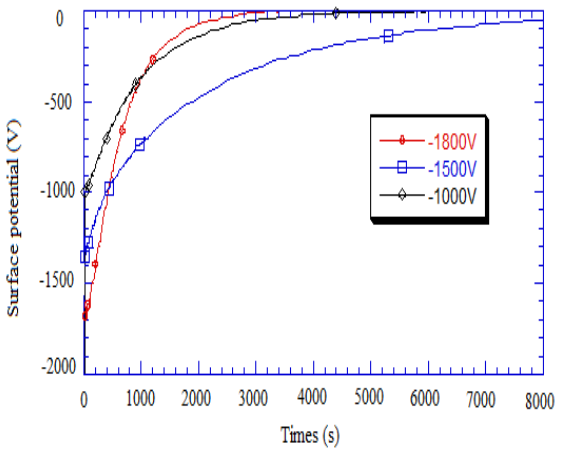


Fig. 2. Surface potential decay curves obtained at three values of the initial potential *V0* at *RH* = 50 % and θ = 55 °C.

The protocol of the experimental tests carried out is described in Table 1 [6].

Table 1. Experimental Test Protocol

	Factors			Responses	
No.	V_0 **(V)**	θ (°C)	***RH*** **(%)**	D_{500} **(%)**	D_{3000} **(%)**
1	-1000	20	50	04.88	20.22
2	-1800	20	50	10.37	29.90
3	-1000	55	50	37.59	94.82
4	-1800	55	50	51.46	99.34
5	-1000	20	80	36.51	89.72
6	-1800	20	80	50.84	97.72
7	-1000	55	80	91.30	100
8	-1800	55	80	99.51	100
9	-1400	37.5	65	45.94	76.64
10	-1400	37.5	65	43.93	76.23
11	-1400	37.5	65	42.92	76.08

3. DIFFERENTIAL EVOLUTION ALGORITHM

As a variant of genetic algorithms, the differential evolution algorithm (DE) is among the most efficient evolutionary algorithms in the field of optimization. DE is an optimization technique that iteratively modifies a population of candidate solutions to converge it to an optimum of your function [17]–[19].

In DE, the solutions are represented as a population of individuals (or vectors). Each individual is represented by a set of real numbers. These real numbers are the values of the parameters of the function to be minimized, which measures the quality of an individual. It is proposed as a simple and powerful population-based stochastic optimization method, which is originally motivated by the mechanism of natural selection. This algorithm searches for solutions using three basic operators: mutation, crossover and greedy selection. Mutation is used to generate a mutant vector by adding differential vectors. After that, crossover operator generates the trial vector by combining the parameters of the mutated vector with the parameters of a parent vector selected from the population. The main difference with genetic algorithms is that it lies in the construction of better solutions where genetic algorithms rely on crossover, firstly, while DE is based on a mutation operation firstly [20]–[23].

Moreover, DE has been proven to be quite efficient when solving real-world problems [24]–[26].

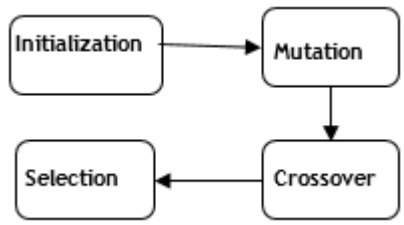


Fig. 3. Block diagram of the DE method.

The main steps of the algorithm are organised according to initializations of the

population, mutation, crossover (recombination), and selection (see Figs. 3 and 4). These operations are applied for minimizing the function f_{obj}.

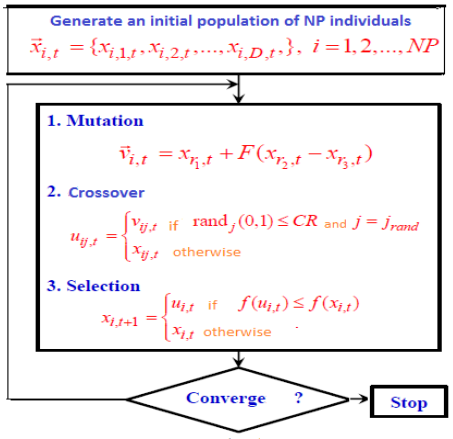


Fig. 4. DE algorithm scheme.

- **Step 1:** We start by generating an initial population where each individual represented by a vector is a candidate solution and its elements are randomly generated, while ensuring compliance with the constraints.
- **Step 2:** A mutant vector is produced $V_{i,t}=x_{r1,t}+F(x_{r2,t} - x_{r3,t})$, where $x_{r1,t}$, $x_{r2,t}$, $x_{r3,t}$, are three candidate solution vectors, distinct, chosen at random among the individuals of the population. F is a random variable $\in$ [0,2].
- **Step 3:** Vector components between X and V are randomly permuted to produce a test vector U. At least one component of V must be exchanged.
- **Step 4:** X is replaced in the population by U only if it is a better candidate (i.e., it better optimizes the "objective" function).

3.1 Improved DE Algorithm

The standard DE algorithm suffers from the fact that it easily falls into the local optimum. In order to get around this problem, we advocate two aspects of modification.

The first aspect concerns the diversification of the initial population through the introduction of the chaotic system concept. The second aspect not only improves diversification but also speeds convergence. Conclusive tests and evaluations were performed on benchmark functions [18].

The first aspect of our proposal is to introduce the concept of Chaos [27], [28]. Chaos has the property of non-repetition and for that it looks for the best solution faster than any search strategy that depends on the probability distribution. It also has a property of ergodicity. The chaotic sequence shows a property of ergodicity that facilitates research. We use a logistic equation to produce the initial population. The logistic mapping equation is as follows:

$$x_{m+1,n} = \mu x_{m,n}\left(1 - x_{m,n}\right) \quad (1)$$

(n=1.2…N ; m = 1.2…M),

when

$x_{m,n} \in [0,1]$ and $0 < \mu \le 4$, the system is at the chaotic state.

$x_{m,n}$ is transformed according to Eq. (1) in order to construct the initial population with a size equal to M and a dimension equal to N.

$$x_{m,n} = L_n + x_{m,n}(U_n - L_n)\,, \quad (2)$$

where

U_n and L_n are respectively the upper limit and the lower limit of the variables or individuals in the n^{th} dimension. The production of a uniform population using logistical chaos mapping can improve the efficiency of the algorithm search.

The second aspect relates to the introduction of a crossing operator that combines

the target vector X with the mutant vector V, according to the following formula:

$$E = \alpha * V_i + (1-\alpha)*X_i, \quad (3)$$

where
$\alpha \in [0,1]$.
At the moment of selection, we took the best individual.

4. PROBLEM FORMULATION

The aim of the study is to find the best coefficients of our polynomial which represents the rate of surface potential decay of PET polyethylene. The linear model of the system response is a polynomial of the first degree, where the response of this process is expressed according to three factors.

$$x_i = V_0^*;\ x_2 = \theta^*;\ x_3 = RH^*$$

$$y = a_0 + a_1 V_0^* + a_2 \theta^* + a_3 RH^* + a_{1,2} V_0^* \theta^* + a_{1,3} V_0^* RH^* + a_{2,3} \theta^* RH^* + a_{1,2,3} V_0^* \theta^* RH^* \quad (4)$$

where
y – the answer or the magnitude of interest. It is measured during the experiment and is obtained with a given precision;
a_0 – the predicted value of the response to the experimental domain centre;
a_i – the factor effect of x_i;
a_{ij} – interaction between factors x_i and x_j;
a_{ijk} – interaction between factors x_i, x_j, x_k.

4.1 The Objective Function (f_{obj})

The "objective" function, or fitness, associates a value for each individual. This value is intended to assess whether an individual is better suited than another to the environment. This means that it quantifies the answer provided to the problem for a given potential solution.

This function depends on the error between the predicted output of the model and the measured experimental value, it is defined by the following relation:

$$Fobj = \frac{1}{N} \sum_{1}^{N} (| y_i - y_{mes} |) \quad (5)$$

where
N – the number of experimental tests;
Y_i – the answer predicted by the model;
Y_{mes} – the measured answer.

4.2 Initialization

The first step of this algorithm is the creation of a population composed of individuals of determinate size. At first, the algorithm initializes individuals by generating random values for each coefficient within given limits.

4.3 Evaluation

At this stage, we have our initial population of 40 vectors and we can now evaluate them using our f_{obj}. Although these vectors are random points in the function space, some of them are better than others. After evaluating these random vectors, we can see the vector that is the best of the population, with minimal f_{obj}, so these values should be closer to those we are looking for.

4.4 Mutation and Recombination

We present here how the algorithm can find a good solution from this set of random values. For each vector X of the population, we take from the population randomly three other vectors: x_{r1}, t, x_{r2}, t, x_{r3}, t. We start with the first initial population vector (called the target vector), and in order to select x_{r1}, t, x_{r2}, t, x_{r3}, t, we first generate a list with the indices of the vectors of the population, excluding the current vector (j = 0); we create a mutant vector combining x_{r1}, t, x_{r2}, t, x_{r3}, t, by calculating the difference between x_{r2}, t and x_{r3}, t by adding these differences to x_{r1}, t after multiplying them by a random mutation factor belonging to l interval [0,1]. A larger mutation factor increases the search radius but may slow the convergence of the algorithm.

In the recombination step, an assay vector composed of a mixture of elements from the mutant vector V and the vector X is created. This is done by changing the elements at certain positions of the current vector with those of the mutant vector.

For each position, we decide (with a probability defined by recomb) whether this element will be replaced or not by that of the mutant at the same position. To generate the crossing points, it is enough to generate uniform random values $\in$ [0, 1] and to check if the values are lower than recomb. After generating our new test vector, we need to evaluate it to measure its quality. If this test vector is better than the target vector X, we replace it with this test vector.

Iteration is accomplished when all vectors of the population have been processed. A certain number of iterations are executed. After every iteration, the best overall solution is determined. At the end of the processing, the vector representing the best overall solution gives the optimal coefficients that minimize the "objective" function.

5. RESULTS

Our approach to solving the problem is based on the improved version of the differential evolution algorithm that we implemented under Python 3.7, using the parameters in Table 2.

Figure 5 illustrates the evolution of the selective function of the best individual for the two time intervals (D_{500s}) and (D_{3000s}). We see a rapid convergence towards the optimal solution.

In addition, we highlight good accuracy of the solution in that the error rate is low (2.77428 % and 1.79136 %).

Table 2. Parameters of DE

Parameters	**Value**
Iteration number with D_{3000}	7000
Iteration number with D_{500}	4000
NP: individual number	40
mutate: probability of the	0.8
recomb: probability of the crossover	0.6

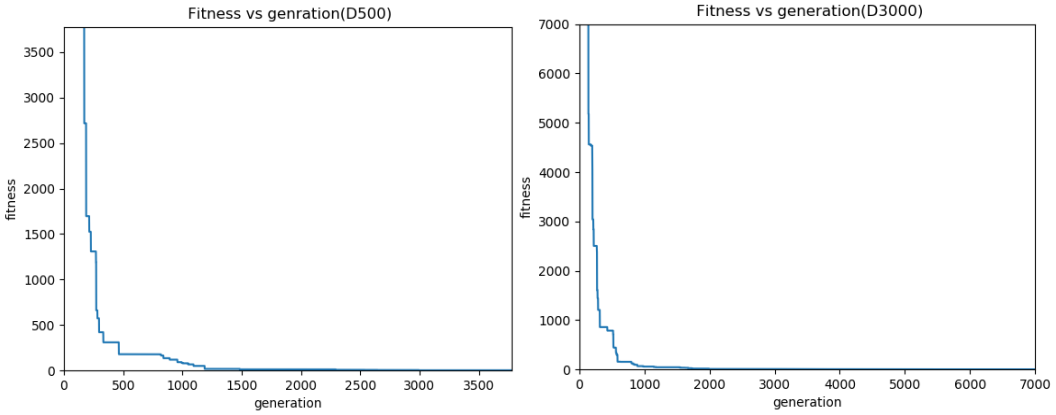


Fig. 5. Evolution of the value of f_{obj} according to the number of generations (D500s) and (D3000s) using DE.

Once the coefficients are determined, the following mathematical models are established:

$$D_{500}= 28\ .613165+0.056946\ V_0^*-2.259979\Theta^*-0.656613RH^*-0.00163\ V_0^*\Theta^*-0.001041\ V_0^*\ RH^*+0.052016\ \Theta^*\ RH^*+2.4^{e-05}\ V_0^*\ \Theta^*\ RH^* \quad (6)$$

$$D_{3000}=49\ .651061+0.099568V_0^*+1.969208\Theta^*+1.237311RH^*-0.00222\ V_0^*\Theta^*-0.001578\ V_0^*RH^*-0.012898\ \Theta^*\ RH^*+3.4^{e-05}\ V_0^*\ \Theta^*\ RH^* \quad (7)$$

Examination of the coefficients of the two polynomial models in the two time intervals shows that the effect of the initial potential factor is less important in relation to the factors: temperature and relative humidity. These have a significant effect on the rate of SPD.

Figure 6 shows iso-response SPD rate curves (D_{500s}, D_{3000s}) as a function of temperature and relative humidity, at V_0 = -1400V, highlighting the important role of these factors and the role of the interaction between them.

This figure shows the importance of temperature and humidity effect on the SPD. It is clear that the two parameters act on the same phenomenon but differently. The effect of temperature appears during the first moments of the decay while the effect of humidity is more widespread over time. The mobility of the electrons strongly depends on the temperature, hence, the appearance of the injection phenomenon from the first moments. This can mean that the action of humidity intensifies the SPD, while the temperature accelerates it.

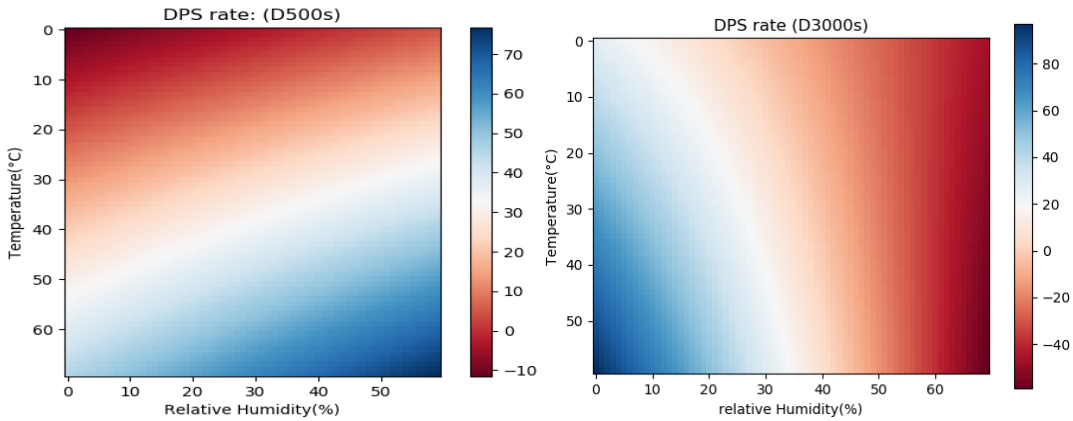


Fig. 6. SPD rate predicted by DE as a function of temperature and the relative humidity RH:(D500 s) and (D3000 s).

Moreover, the predicted response curves computed with Eqs. (6) and (7) and represented in Figs. 7 and 8 can also determine the influence of each factor on the response by plotting the variation of the responses according to the factors. In each case, the other two variables are held constant and equal to their central values V_0 = -1400 V, Θ = 37.5 °C, *RH* = 65 %.

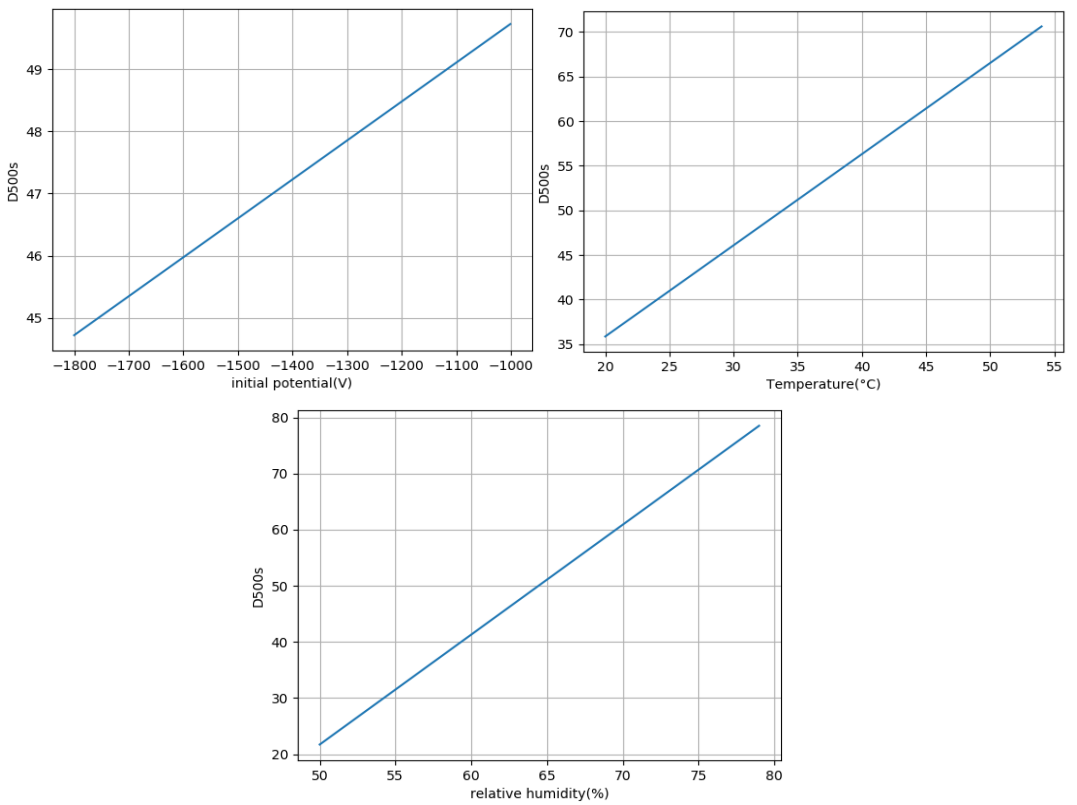


Fig. 7. Predicted responses (D500) with DE according to factors: *V0* and *RH*.

If we consider the effect of each factor on the DPS rate, we note that the fall is very important, it depends strongly on the temperature and the relative humidity for the first linear model, D_{500s} (see Fig. 7).

This behaviour can be explained by the fact that at the first moment of measurements the high decay rate and consequently the high sample unloading speed can be attributed to the charge injection mechanism. The injected charges are subject to the local field, which will drive them towards the rear face. In the long term D_{3000s} (500s–3000s) (Fig. 8), it seems that the effect of both factors whether it is temperature or relative humidity on the DPS becomes less important than the short term D_{500s}.

It is also important to note that the recorded surface potential decline is more significant, especially in the first moments of measurement (~ 500s). For long periods, a very slow or even stationary decline is observed, it is possible that the charges do not have enough energy to be injected into the volume of the material. The deep states of the surface permanently trap part of the deposited charge.

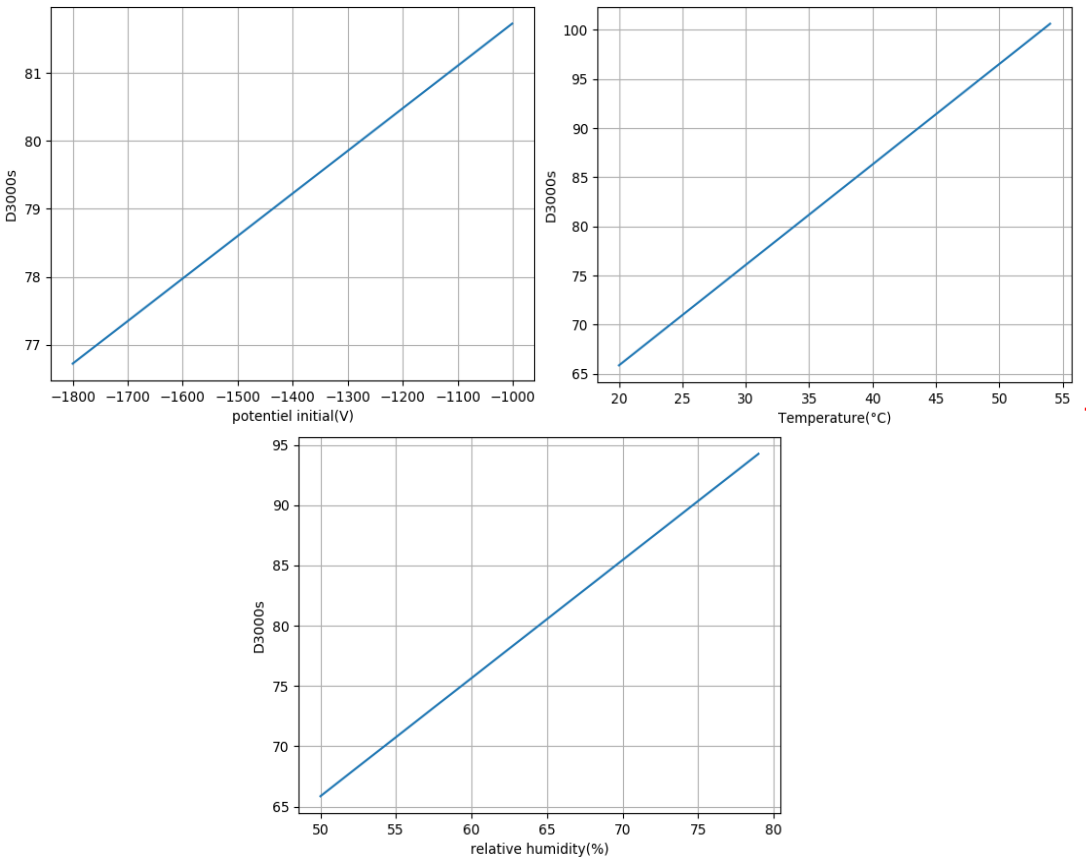


Fig. 8. Predicted responses (D3000) with DE according to factors: (*V0*, and *RH*).

6. VALIDATION

Let us recall that we divided the experimental data set into two parts: the first part, which represents 80 %, was used for the determination of the coefficients by the improved differential evolution algorithm (DEA). The remaining 20 % was used to validate our model. By replacing the three factors in the found mathematical models, one calculates the rate of decline D_t of the corresponding (D_{500s} and D_{300s}), then one compares it with the experimental one. The results obtained (see Table 3) show a very slight difference, which signifies a very good quality of the results obtained and hence the efficiency of our algorithm that improves differential evolution optimization method. Therefore, both models fit well the experimental data, and enable accurate prediction of the surface potential decay rate.

Compared to the results obtained by genetic algorithms, it is quite clear that the improved differential evolution algorithm more accurately determines the rate of potential decay for the two periods D_{500s} and D_{3000s}.

In order to show the superiority of our approach, we compared the results obtained by applying genetic algorithms with those obtained by our technique. This superiority is materialized as much by the execution time as by the precision of the results. Table 4 illustrates this comparison.

Table 3. Validation Results of Mathematical Models with DE

	Predicted value	Experimental value	Precision	Excution time
$\mathbf{D_{500}}$	44.52516	45.94	0.9692	52 s
$\mathbf{D_{3000}}$	73.08340	76.64	0.9535	95 s

Table 4. Validation Results of Mathematical Models with GA

	Predicted value	Experimental value	Precision	Execution time
$\mathbf{D_{500}}$	38.87431	45.94	0.8461	112 s
$\mathbf{D_{3000}}$	67.33452	76.64	0.8806	185 s

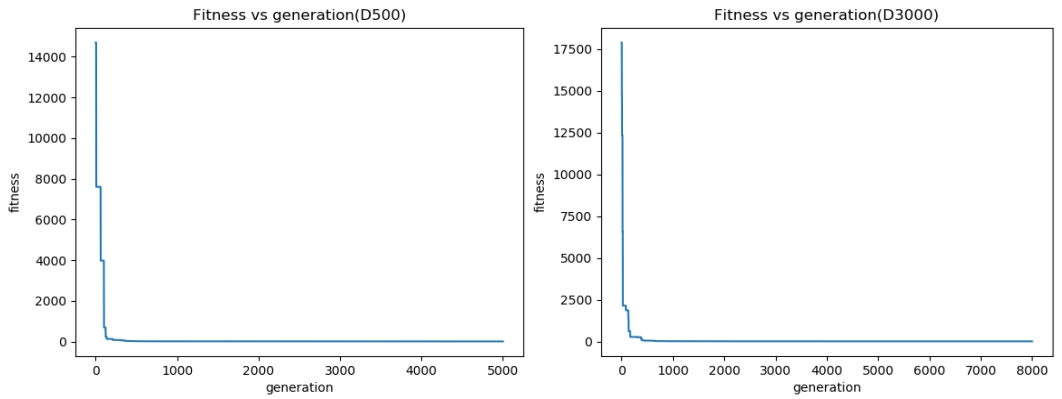


Fig. 9. Evolution of the value of f_{obj} according to the number of generations (D500 s) and (D3000 s) obtained by GA.

Figure 9 illustrates the evolution of the "objective" function by the number of generations. It shows that in the short term (D_{500s}) the genetic algorithm reaches the best solution in the 1500 generation after 112 s. In the long term (D_{3000s}), the algorithm reaches the best solution at the 3200 generation after 185 s; this is much compared to that obtained by our DEA algorithm.

7. CONCLUSION

Applications in electrical engineering use insulation systems that are often a limiting factor in performance, especially for service life or voltage withstand; hence, they need to be improved and there should be an opportunity to predict their lifetime.

In this study, we defined the mathematical model of SPD characterisation, to which we applied the improved and adapted differential evolution algorithm. It allowed not only quantifying the effect of each factor but also determining the interaction between them. The developed algorithm has a great flexibility of use and may handle large problems. It has been proven powerful for optimizing complex functions and can work well in problems where other techniques cannot be used.

Compared to the genetic algorithm, it exhibited lower computation time than that of the genetic algorithm. Moreover, it allows for a better result in terms of precision and estimation of the coefficients of the mathematical models for the problem of the decline in surface potential.

This leads to the belief that in the future our modified version of the differential evolution algorithm will be able to solve problems related to modelling and optimization of experimental work with increased complexity (non-linearity).

REFERENCES

1. Moreno, R.A., & Gross, B. (1976). Measurement of Potential Buildup and Decay, Surface Charge Density, and Charging Currents of Corona-Charged Polymer Foil Electrets. *J. Appl. Phys., 47* (8), 3397–3402.
2. Batra, I.P., Kanazawa, K.D., & Seki, H. (1970). Discharge Characteristics of Photoconducting Insulators. *J. Appl. Phys., 41* (8), 3416–3422.
3. Vance, D.W. (1971). Surface Charging of Insulators by Ion Irradiation. *J. Appl. Phys, 42* (13), 5430–5443.
4. Young, R.H. (1992). Kinetics of Xerographic Discharge by Surface Charge Injection. *J. Appl. Phys*, *72* (7), 2993–3004.
5. Ieda, M., Sawa, G., & Shinohara, I. (1967). A Decay Process of Surface Electric Charges across Polyethylene Film. *Japan. J. Appl. Phys, 6*, 793–794.
6. Herous, L., Nemamcha, M., Remadnia, M., & Dascalescu, L. (2009). Factors that Influence the Surface Potential Decay on a Thin Film of Polyethylene Terephthalate (PET). *Journal of Electrostatics, 67*, 198–202.
7. Herous, L., Remadnia, M., Kachi, M., & Nemamcha, M. (2009). Decay of Electrical Charges on Polyethylene Terephthalate Surface. *Journal of Engineering Science and Technology Review, 2* (1), 87–90.

8. Smili, K., & Herous, L. (2019). Corona Charging and Charge Decay on Polyethylene Terephthalate Films (PET). *Electrotehnica, Electronica, Automatica (EEA), 67* (3), 81–90. ISSN 1582-5175.
9. Remadnia, M., Nemamcha, M., Herous, L., & Dascalescu, L. (2011). Decay of the Electrical Potential at the Surface of Corona Charged Uniforms Layers of HIPS Granules. *IEEE Transactions on Dielectrics and Electrical Insulation, 18* (2), 579–587.
10. Kasri, S., & Herous, L. (2018). Neuronal approach for estimating surface potential decay in polyethylene terephthalate. In: Proceeding of the 3rd International Conference on Technological Advances in Electrical Engineering (ICTAEE'18), (pp. 392–397). 10–12 December 2018, Skikda, Algeria.
11. Kasri, S., & Herous, L. (2018). Modeling the potential surface decay of a polymer (PET) using artificial neural networks. In: Proceeding of the 4th International Organic Chemistry Days, (p. 180). 1–3 December 2018, ANNABA, Algeria.
12. Mizutani, T., Oomura, T., & Ieda, M. (1989). Surface Potential Decay in Polyethylene. *Japan. J. Appl. Phys, 20*, 855–859.
13. Rougdia, K., Herous, L., Fatihou, A., Tabti, B., Nemamcha, M., & Dascalescu, L. (2015). Experimental Modelling of the Electric Potential Decay at the Surface of Polypropylene. *Journal of Electrostatics, 76*, 262–267.
14. Rouagdia, K., Nemamcha, M., Herous, L., Dascalescu, L., & Mellouki, H. (2015). Surface Potential Decay of DC-corona-charged PET Films on Humid Electrodes. *Journal of Electrostatics, 78*, 17–21.
15. von Berlepsch, H. (1985). Interpretation of Surface Potential Kinetics in HD-PE by a Trapping Model. *J. Phys. D: Appl. Phys., 18*, 1155.
16. Llovera, P., "Study of charge injection mechanisms in insulating materials by means of electrostatic measurements of potential decline and return, New analysis tools ", thesis PhD University of Paris XI Orsay, 2002.
17. Price, K. V., Storn, R. M., & Lampinen, J. A. (2014). *Differential Evolution: A practical Approach to Global Optimization*. Springer.
18. Derviş, K., & Selçuk, Ö. (2004). A Simple and Global Optimization Algorithm for Engineering Problems: Differential Evolution Algorithm. *Turkish Journal of Electrical Engineering and Computer Science (TUBITAK), 12* (1), 53–60.
19. Storn, R., & Price, K. (1997). Differential Evolution - A Simple and Efficient Heuristic for Global Optimization over Continuous Spaces. *Journal of Global Optimization*, 341–359.
20. Huanzhe, L., Kungi, L., & Xia, L. (2010). A Comparative Study of Artificial Bee Colony, Bees Algorithm and Differential Evolution on Numerical Benchmark Problems. *Appl Math Comput., 107*, 198–207.
21. Canessa, E., & Chaigneau, S. (2017). Response Surface Methodology for Estimating Missing Values in a Pareto Genetic Algorithm Used in Parameter Design. *Ingeniería e Investigación, 37* (2), 89–98.
22. Bentouati, B., Chettih, S., & Esehiemi, R. (2017). A Chaotic Firefly Algorithm for Non-convex Economic Dispatch Problem. *Electrotehnica, Electronica, Automatica (EEA), 60* (1), 172–179. ISSN 1582-5175.
23. Eiben, A.E., & Smith, J.E. (2015). *Introduction to Evolutionary Computing* (2nd ed.) Berlin: Springer Verlag, Heidelberg.
24. Zhang, Y., & Zhou, D. (2016). Application of differential evolution algorithm in future collider optimization. In: Proceedings of IPAC'16 (pp. 2–4). 8–13 May 2016, BEXCO, Busan Korea.
25. Zhao, J., Li, T., & Ian, J. (2005). Application of particle swarm optimization algorithm on robust PID controller tuning. In: Advances in Natural Computation (ICNC). 27–29 August 2005, Changsha, China. Heidelberg: Springer-Verlag Berlin.
26. Karaboga, D., & Okdem. S. (2016). A Modified Artificial Bee Colony (ABC) Algorithm for Constrained Optimization Problems. *Applied Soft Computing, 11* (3), 3021–3031.

27. Sheikholeslami, R., & Kaveh, A. (2013). A Survey of Chaos Embedded Meta-Heuristic Algorithms. *Int. J. Optim. Civil. Eng., 3* (4), 617–633.

28. Wen, H., Hou, S., Liu, Z., & Liu, Y. (2017). An Optimization Algorithm for Integrated Remanufacturing Production Planning and Scheduling System. *Chaos, Solutions & Fractals, 105*, 69–76.